8052 *Macromolecules* **2009**, *42*, 8052–8061
DOI: 10.1021/ma901706u

Macromolecules
ARTICLE

Multifunctional Hyperbranched Oligo(fluorene vinylene) Containing Pendant Crown Ether: Synthesis, Chemosensory, and Electroluminescent Properties

Juin-Meng Yu and Yun Chen*

Department of Chemical Engineering, National Cheng Kung University, Tainan, Taiwan

Received July 31, 2009; Revised Manuscript Received September 8, 2009

ABSTRACT: Multifunctional hyperbranched oligo(fluorene vinylene) (**HOFC**) containing pendant crown ether was synthesized from 2,4,7-trivinyl-9,9-dihexylfluorene and 2,7-dibromo-9-(15-crown-4)-9*H*-fluorene via Heck coupling reaction. Their chemosensory, photophysical, and electrochemical properties were investigated and compared with those of linear oligo(fluorene vinylene) (**LOFC**) to elucidate the effect of hyperbranched structure. Both **HOFC** and **LOFC** exhibit selective fluorescence quenching toward Fe^{3+} and Ru^{3+}, with the Stern−Volmer coefficients (K_{sv}) to Ru^{3+} being 2×10^4 and 1.9×10^4 M^{-1}, respectively. The stability constant (K_s) of forming complex with Ru^{3+} are 3.1×10^3 and 5×10^3 M^{-1} for **HOFC** and **LOFC**. Moreover, hyperbranched **HOFC** reveals homogeneous film morphology due to its hyperbranched structure. After thermal treatment, the cured polymer (**HFC**) shows better thermal stability because of higher cross-linked density. Double-layer electroluminescent devices (ITO/PEDOT:PSS/**HFC** or **LFC**/Ca/Al), using thermally cross-linked **HFC** or **LFC** as emitting layer, were fabricated to investigate their optoelectronic properties. The turn-on voltage, maximum luminance and maximum luminance efficiency of **HFC** device (4.1 V, 7132 cd/m^2 and 1.3 cd/A) are superior to those of **LFC** device (6.2 V, 331 cd/m^2, 0.22 cd/A), which have been attributed to its homogeneous film morphology. Current results indicate that the hyperbranched oligo(fluorene vinylene) is a promising material for chemosensors and electroluminescent devices.

Introduction

Conjugated polymers have attracted considerable attention among scientists due to their potential applications in light-emitting diodes (LEDs),[1,2] chemical sensors,[3,4] organic solar cells,[5,6] and field-effect transistors.[7,8] The great advantages of polymer light-emitting diodes (PLEDs) are tunable emission color through molecular design and solution-processable by appropriate derivation, which are suitable for large-area-display devices by spin-coating or printing methods. In PLEDs, polyfluorenes (PFs) are the most widely applied as blue-emitting material due to its high photoluminescence (PL), chemical and thermal stability, high quantum yield, solubility, and facile property modification via substitution at C-9 of fluorene unit.[9,10] However, the PFs still show some drawbacks that restrict their potential applicability, such as undesirable green emission upon thermal treatment or device operation, which has been attributed to the formation of interchain interaction (excimer or aggregate formation) in solid state or ketonic defects.[11−13] There are numerous ways proposed to minimize the interchain interaction, such as introducing or end-capping with bulky groups in the side chain or the end of polymer chain, respectively,[14−16] kinking backbone structure,[17,18] and hyperbranched construction.[19,20]

Hyperbranched polymers, a transitional structure of linear polymers and dendrimers, own many branches on their backbones. They are not only easier to synthesize (sometimes only one step is needed), but also possess properties comparable to dendrimers. A hyperbranched polymer comprises three parts: the core, the connecting unit and the terminal group. Some of the advantages of hyperbranched polymer are lower intrinsic viscosity, improved solubility, and easeness in processing, which are originated from their highly branched and globular molecular structure.[21] Stable amorphous film is readily obtainable from the hyperbranched polymers owing to reduced interchain cohesive force, when compared with analogous linear counterparts. The amorphous and homogeneous morphology in the emitting layer is critical in PLED device fabrication because it contributes beneficially to performance enhancement.[21−24] In addition, hyperbranched polymers, prepared by Heck coupling or Witting reaction, may possess many reactive functional groups through controlling stoichiometry of the feed monomers; for instance, styryl-functionalized oligomers have a lot of reactive vinyl end-groups, which are promising candidates of thermal cross-linkable precursor.[25−27] Hyperbranched oligomers own more terminal vinyl groups than linear counterparts, leading to higher cross-linking density after heat treatment. The thermally cured polymers should possess better solvent resistance and thermal stability that are highly required in fabricating PLED devices.

Conjugated polymers-based fluorescent sensors have emerged as an important chemical sensory material due to its high sensitivity in transforming chemical signal into electrical or optical signals upon binding with analyte.[28,29] The high sensitivity is mainly acquired by the highly conjugated backbone through which the signal is transformed and amplified. A chemosensor is usually comprised of a recognition moiety and a signal transducer group. The signal transducer converts the information, caused by the interaction between recognition moiety and analyte, into an optical signal and is expressed as changes in photophysical characteristics of the fluorophore. Comparing to small molecules, conjugated polymers is able to produce signal gain in response to interactions with analytes, resulting in the amplification of fluorescent signals.[30] Due to their high sensitivity and ease of measurement, conjugated polymers have serviced as a major stream in the next generation. Moreover, introducing a recognition moiety into

*Corresponding author. Telephone: +886-6-2085843. Fax: +866-6-2344496. E-mail: yunchen@mail.ncku.edu.tw.

 Published on Web 09/21/2009

polyfluorene can result in a promising multifunctionalized conjugated polymer, in which can be applied in both the chemical sensor and the PLED emitter.

In this article, we synthesized a new trivinylfluorene (**3**) as branching monomer and copolymerized it with crown ether-containing fluorene (**5**) via Heck coupling reaction to give a multifunctionalized conjugated hyperbranched oligomer. The oligomer shows high selective response toward specific metal cations (Fe^{3+}, Ru^{3+}) and thermally cross-linkable character. The latter was examined by differential scanning calorimeter (DSC) to evaluate their curing behaviors. After thermal curing, the hyperbranched polymer demonstrated homogeneous film, good solvent resistance, and high thermal stability. Moreover, its electroluminescent performance is also superior to those of linear counterpart.

Experimental Section

Material. 9,9-Dihexylfluorene and compounds **1**, **2**, **4**, and **5** were synthesized according to the procedures reported previously.[31−33,35] Syntheses of compounds **1** and **2** are described in the Supporting Information. Hydrogen bromide solution (33 wt %) in glacial acetic acid, formaldehyde aqueous solution (37 wt %), tri-(*o*-tolyl)phosphine, tributylamine, and potassium *tert*-butoxide were procured from Acros Co. and used as received. 1-Bromohexane, fluorene, and tetra-*n*-butylammonium bromide were acquired from Alfa Aesar Co. Palladium(II) acetate, paraformaldehyde, and 9,9-dihexyl-2,7-dibromofluorene was purchased from Wako Co., Showa Co., and Aldrich Co., respectively, and used without further purification. *N*,*N*-Dimethylformamide (DMF) and other reagents were used without further purification except specifically notified.

Instrumentations. All synthesized compounds were identified by ^{1}H NMR, ^{13}C NMR, and elemental analysis (EA). The ^{1}H and ^{13}C NMR spectra were recorded on a Bruker AMX-400 MHz FT-NMR, and the chemical shifts are reported in ppm using tetramethylsilane (TMS) as an internal standard. The elemental analysis was carried out on a Heraus CHN-Rapid elemental analyzer. The thermogravimetric analysis (TGA) was performed under a nitrogen atmosphere using a Perkin Elmer TGA-7 thermal analyzer at a heating rate of 20 °C/min. The thermal curing behaviors and thermal transitional properties of the oligomers and polymers were recorded using a differential scanning calorimeter (DSC), Mettler DSC 1, with a heating rate of 20 °C/min. Absorption and photoluminescence (PL) spectra were measured on a Jasco V-550 spectrophotometer and a Hitachi F-4500 spectrofluorometer, respectively. Cyclic voltammograms were measured with a voltammetric apparatus (model CV-50W from BAS) equipped with a three-electrode cell. The cell was made up of an oligomer-coated glassy carbon as the working electrode, an Ag/AgCl electrode as the reference electrode, and a platinum wire as the auxiliary electrode. The electrodes were immersed in acetonitrile containing 0.1 M (n-Bu)$_4$NClO$_4$. The energy levels were calculated using the ferrocene (FOC) value of −4.8 eV with respect to vacuum level, which is defined as zero.[34] An atomic force microscope (AFM), equipped with a Veeco/Digital Instrument Scanning Probe Microscope (tapping mode) and a Nanoscope IIIa controller, was used to examine the morphology and to estimate the root-mean-square roughness (rms) and thickness of deposited films.

Preparation of Metal Ion Solutions and Titration. The chloride salts of Li^+, Na^+, Cu^+, Ca^{2+}, Zn^{2+}, Ce^{3+}, Ge^{4+}, Fe^{3+}, and Ru^{3+} were dissolved in a mixture solvent of DMF/H_2O (87.8/12.2, v/v) to prepare their corresponding stock solutions (2.2×10^{-4} M). Titration was done by adding 9 mL of the metal ion solution (2.2×10^{-4} M) to a test tube with 1 mL of oligomer solution (10^{-5} M in DMF). All of the optical measurements were operated right after the test solutions were prepared and thoroughly mixed. The Stern−Volmer constant (K_{sv}) and stability constant (K_s) were obtained according to the fluorescent data and the using equations were described in Supporting Information.

Fabrication of Electroluminescent Devices. Double-layer light-emitting diodes with a configuration of ITO/PEDOT:PSS/cross-linked polymer/Ca/Al were fabricated to investigate their optoelectronic characteristics. The ITO-coated glasses were washed successively in ultrasonic baths of neutraler reiniger/deionized water (1:3 v/v) mixture, deionized water, acetone, and 2-propanol, followed with cleaning in a UV−O_3 chamber. A thick hole-injection layer of PEDOT:PSS was spin-coated on top of the cleaned ITO glass and annealed at 150 °C for 15 min in a dust-free atmosphere. Upon the hole injecting PEDOT:PSS layer was spin-coated with an emitting layer from an oligomer solution in chlorobenzene (20 mg/mL, 2000 rpm) and heated at 180 °C for 1 h under a nitrogen atmosphere. The oligomer solutions were filtered through a syringe filter (0.2 μm) before the spin-coating. Finally, a thick layer of Ca and Al were successively deposited as cathode via vacuum deposition under 1×10^{-6} Torr. The luminance-bias, current density-bias, and EL spectral characteristics of the devices were recorded using a combination of Keithley power source (model 2400) and Ocean Optics usb2000 fluorescence spectrophotometer. The fabrication of the devices was done in ambient conditions, with the following performance tests conducted in a glovebox filled with nitrogen.

Synthesis of 2,4,7-Trivinyl-9,9-dihexylfluorene (3). To a mixture of compound **2** (2.8 g, 2 mmol), 37 wt % formaldehyde aqueous solution (2.22 g, 74 mmol) and 5 mL of water was added with 5 mL of NaOH aqueous solution (17 wt %) dropwise (Scheme 1). The mixture was stirred at room temperature for 18 h under a nitrogen atmosphere, followed by extracting with diethyl ether. After removal of diethyl ether by a rotary evaporator, it was purified by column chromatography using *n*-hexane as eluent to afford a colorless liquid of **3** (0.62 g, 75.2%). ^{1}H NMR (400 MHz, $CDCl_3$, TMS, 25 °C): δ 7.79−7.77 (d, 1H, J = 8.4 Hz), 7.5−7.3 (m, 4H, Ar−H), 7.28 (s, 1H, Ar−H), 6.8−6.7 (m, 2H, =CH−), 5.8−5.7 (m, 3H, =CH−), 5.48−5.45 (d, 1H, =CH_2, J = 12 Hz), 5.29−5.25 (dd, 2H, =CH_2, J_1 = 12 Hz, J_2 = 8 Hz), 1.97−1.93 (m, 4H, −CH_2−), 1.25−0.56 (m, 22H, −CH_2−). ^{13}C NMR (400 MHz, CDCl3, TMS, 25 °C): δ 151.9, 151.8, 141.1, 137.7, 137.2, 137.1, 136.2, 136, 135.6, 134, 125.2, 123.9, 123.1, 120.2, 119.3, 116.6, 113.3, 113.2, 54.2, 40.7, 31.4, 29.6, 23.5, 22.5, 13.98. Anal. Calcd for $C_{31}H_{40}$: C, 90.23; H, 9.77. Found: C, 90.07; H, 9.89.

Synthesis of 2,7-Divinyl-9,9-dihexylfluorene (4).[33]**.** To a 25 mL glass reactor were added 2,7-dibromo-9,9-dihexylfluorene (0.406 g, 0.82 mmol), tributylvinyltin (0.575 g, 1.8 mmol), $PdCl_2(PPh_3)_2$ (0.046 g, 0.07 mmol), and 10 mL of toluene. The mixture was refluxed for 1 day under a nitrogen atmosphere. After cooling to room temperature, diethyl ether (20 mL) and KF solution (10 wt %, 10 mL) was added and the solution was stirred for 1 day. The organic layer was collected and washed with water, followed by drying over anhydrous magnesium sulfate. After removal of the solvent by a rotary evaporator, it was purified by column chromatography using *n*-hexane as eluent to afford colorless liquid of **4** (0.2 g, 62.8%). ^{1}H NMR (400 MHz, $CDCl_3$, TMS, 25 °C): δ 7.61−7.59 (d, 2H, J = 8 Hz, Ar−H), 7.38−7.33 (m, 4H), 6.8−6.7 (m, 2H), 5.8−5.76 (d, 2H, J = 16 Hz), 5.26−5.22 (d, 2H, J = 16 Hz), 1.97−1.93 (m, 4H), 0.6−1.4 (m, 22H). ^{13}C NMR (400 MHz, $CDCl_3$, TMS, 25 °C): δ 151.3, 140.7, 137.4, 136.4, 125.2, 120.4, 119.6, 112.9, 54.8, 40.4, 31.4, 29.6, 23.6, 22.56, 14.9. Anal. Calcd for $C_{29}H_{38}$: C, 90.09; H, 9.91 Found: C, 89.29; H, 10.10.

Synthesis of Hyperbranched (HOFC) and Linear Oligomers (LOFC). As shown in Scheme 2, hyperbranched (**HOFC**) and linear (**LOFC**) oligo(fluorene vinylene)s were prepared from trivinyl (**3**) and divinyl (**4**) fluorene monomers, respectively, by coupling (Heck reaction) with crown ether-containing dibromofluorene (**5**). For example, to a 15 mL glass reactor were added with **3** (0.12 g, 0.3 mmol), **5** (0.14 g, 0.27 mmol), $Pd(OAc)_2$

Scheme 1. Synthetic Routes of Branching (3) and Linear (4) Monomers

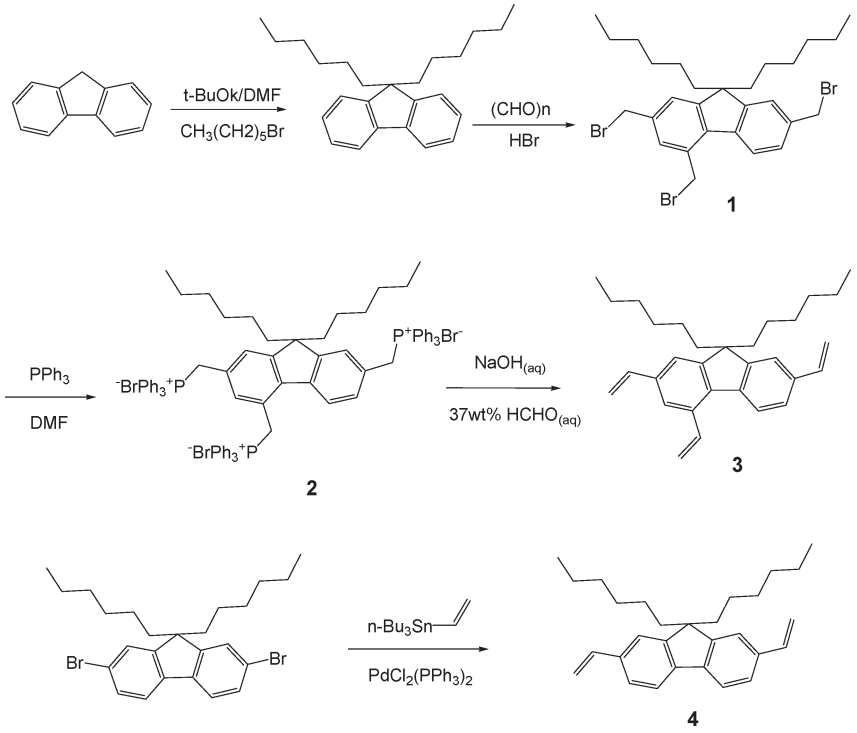

(60 mg, 0.27 mmol), tri*o*-tolylphosphine (0.24 g, 0.81 mmol), tributylamine (0.1 g, 0.54 mmol), K_2CO_3 (41 mg, 0.3 mmol), and a mixture solvent of DMF/toluene/H_2O = 6/4/0.5 (v/v/v). The mixture was stirred at 90 °C for 40 min. After adding a mixture of compound **3** (0.12 g, 0.3 mmol) and styrene (0.163 g, 1.56 mmol) as the end-capping agent, the polymerization was proceeded for an additional 10 min. The solution was poured into a large amount of methanol and the appearing precipitate was collected by filtration and dried in vacuo at room temperature for 1 day to afford **HOFC** (yield: 25%). The linear oligo(fluorene vinylene) (**LOPC**) was prepared by analogous procedures, using divinylfluorene (**4**) instead of trivinylfluorene (**3**). The reaction time was 17 h at 90 °C, followed by additional 1 h for end-capping reaction at the same temperature (yield: 42%).

HOFC. ^{1}H NMR (400 MHz, $CDCl_3$, TMS, 25 °C): δ 7.82−7.12 (m, Ar−H and =CH−), 6.85−6.65 (m, =CH−), 5.88−5.80 (m, $=CH_2$), 5.56−5.51 (m, $=CH_2$), 5.31−5.25 (m, $=CH_2$), 3.8−3.4 (m, 16H, $-CH_2-$), 2.49−2.39 (m, 4H, $-CH_2-$), 2.0 (m, 4H, $-CH_2-$), 1.2−0.7 (m, 22H, $-CH_2-$ and $-CH_3$). ^{13}C NMR (400 MHz, $CDCl_3$, TMS, 25 °C): δ 151.5, 139.2, 137.5, 136.6, 136.4, 136.2, 136, 135.8, 134.2, 129.1, 128.7, 128.2, 127.5, 127.1, 126.4, 125.6, 124.2, 123.3, 121.7, 120.4, 120.1, 119.6, 116.7, 70.6, 60.1, 68.5, 54.3, 52.1, 40.9, 40.8, 38.4, 38.3, 31.5, 29.8, 23.7, 22.63, 14. Anal. found (%) for **HOFC**: C, 78.5; H, 7.76.

LOFC. ^{1}H NMR (400 MHz, $CDCl_3$, TMS, 25 °C): δ 7.85−7.11 (m, Ar−H and =CH−), 6.9−6.75 (m, =CH−), 5.83−5.79 (m, $=CH_2$), 5.56 (m, $=CH_2$), 5.28−5.25 (m, $=CH_2$), 3.8−3.3 (m, 16H, $-CH_2-$), 2.7−2.35 (m, 4H, $-CH_2-$), 2.0 (m, 4H, $-CH_2-$), 1.2−0.7 (m, 22H, $-CH_2-$ and $-CH_3$). Anal. Calcd for **LOFC**: C, 83.1; H, 8.3. Found: C, 80.1; H, 8.1.

Result and Discussion

Synthesis and Characterization of Monomer (3) and Oligo(fluorene vinylene)s. Tribromomethyl fluorene (**1**) had been synthesized and characterized in our previous study.[35] The key monomer 2,4,7-trivinyl-9,9-dihexylfluorene (**3**) was successfully synthesized from triphenylphosphonium derivative (**2**) and formaldehyde using sodium hydroxide as alkaline catalyst (Scheme 1). Figure 1 shows the ^{1}H NMR spectra of monomer **3**, in which chemical shifts at 5.25−5.80 ppm have been assigned to protons of vinyl substituents. The ratio of peak area of 2,7-vinyl (g) over that of 4-vinyl (f) is roughly 2/1, consistent with the structure of 2,4,7-trivinyl-9,9-dihexylfluorene (**3**). Figure 2 is the corresponding ^{13}C NMR spectra of monomer **3** and the peaks located at 113.3−113.2 ppm (l) and 116 ppm (s) have been assigned to vinyl carbons at 2,7- and 4-vinyl substituents, respectively. The structure of **3** was satisfactorily characterized by ^{1}H and ^{13}C NMR spectra and elemental analysis. The 2,4,7-trivinyl-9,9-dihexylfluorene (**3**) is a new trifunctional monomer, which is applicable as branching unit in synthesizing hyperbranched polymers. Monomer **5** was synthesized from triethyleneglycol ditosylate and 9,9-dihydroxyfluorene under high dilute conditions and had been reported in our previous study.[32] Incorporation of crown ether moiety provides the ability to capture metal ions to form as complex. Accordingly, the resulting conjugated oligo(fluorene vinylene)s or poly(fluorene vinylene)s might be applied not only as electroluminescent material but also as polymer-based chemosensor.

Hyperbranched oligo(fluorene vinylene) containing pendant crown ether groups (**HOFC**) was successfully synthesized from monomer **3** and **5** via the Heck coupling reaction using $Pd(OAc)_2$ as the catalyst. However, because residual terminal bromo groups are detrimental to light-emitting application, a mixture of trivinylfluorene monomer **3** and styrene was therefore employed to react with the terminal bromo groups to transfer them into vinyl or phenyl groups. The weight-average molecular weights (M_w) of oligomers **HOFC** and **LOFC**, as determined by gel permeation chromatography using monodisperse polystyrene as standard, was 8.4×10^3 and 2.5×10^3, with the polydispersity indexes (PDI) being 1.6 and 1.3 (Table 1), respectively. Due to polar nature of the crown ether moiety, the resulting oligomers are readily soluble not only in common organic solvent such as

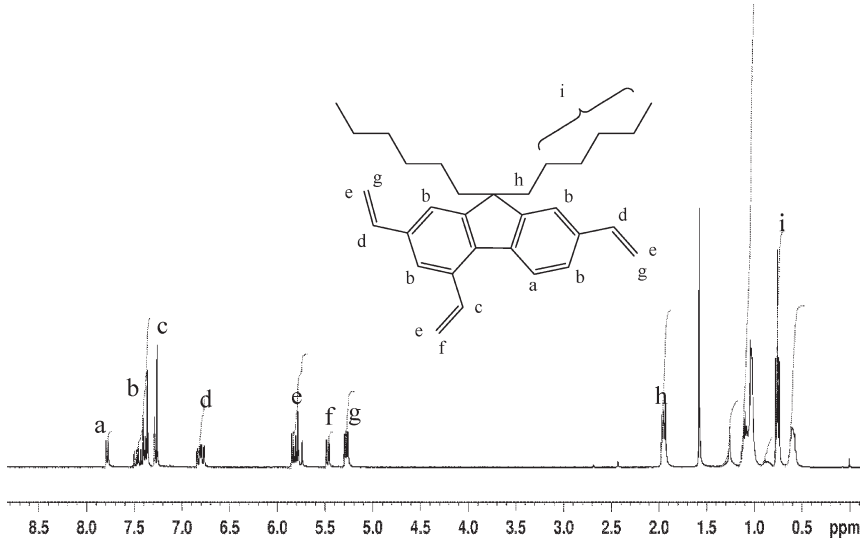

Figure 1. ^{1}H NMR spectrum of 2,4,7-trivinyl-9,9-dihexylfluorene (**3**) dissolved in $CDCl_3$. The chemical shifts are reported in ppm using tetramethylsilane (TMS) as an internal standard.

Scheme 2. Synthesis and Thermal Cross-Linking of Hyperbranched (HOFC) and Linear Oligomers (LOFC)

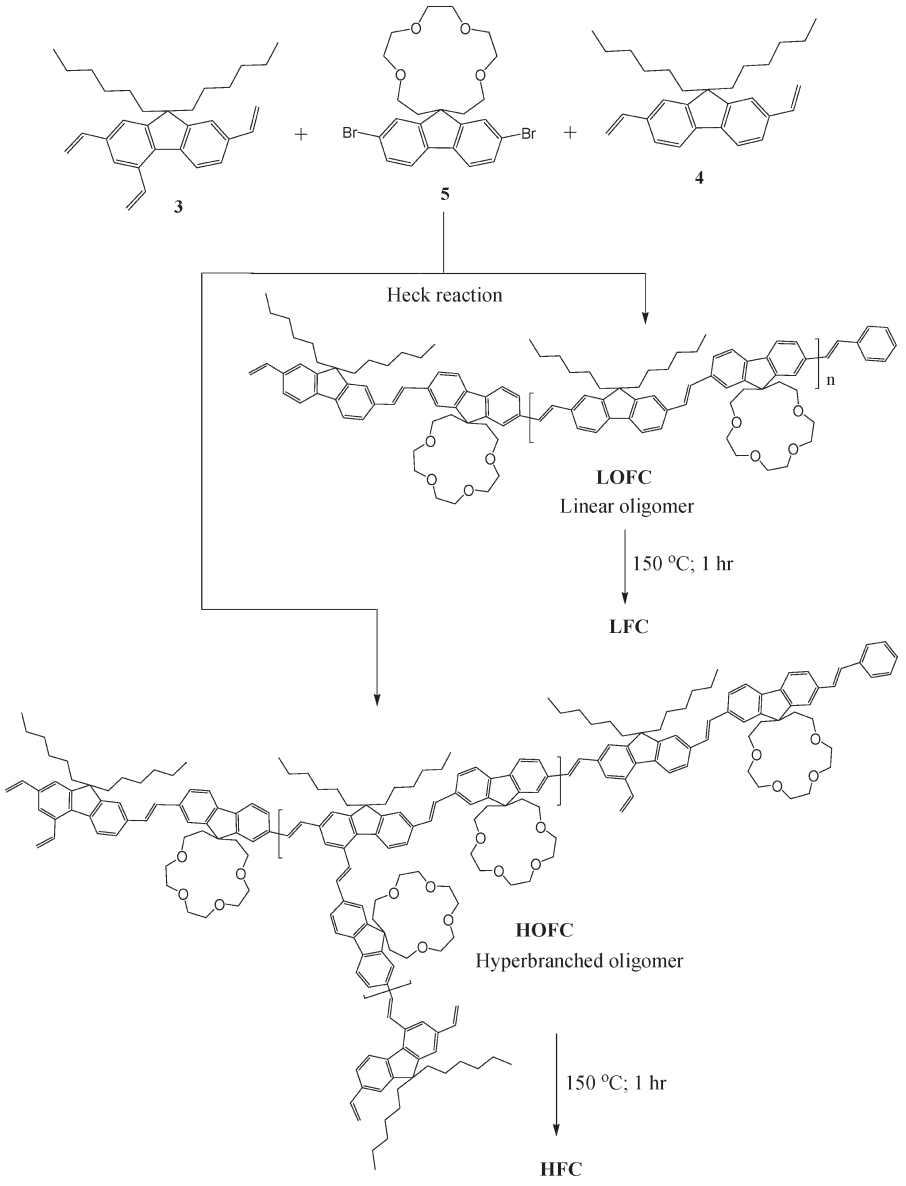

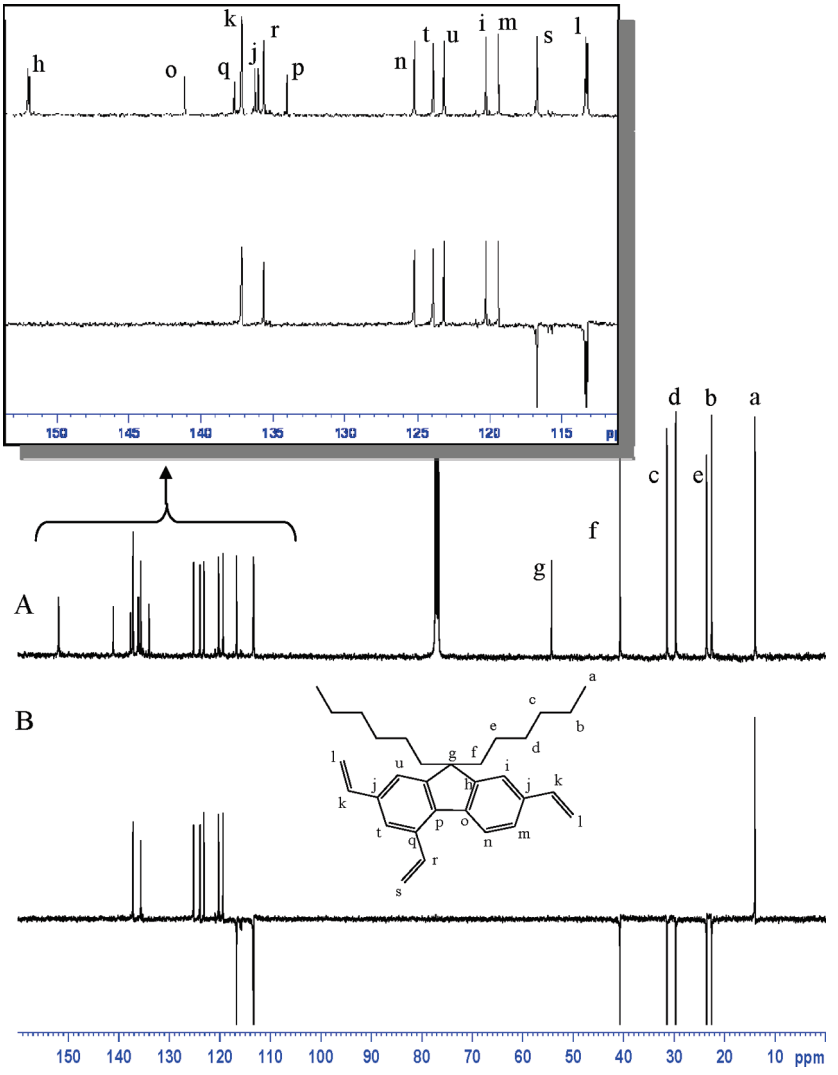

Figure 2. ^{13}C NMR spectrum (A) and DEPT (distortionless enhancement by polarization transfer) (B) of 2,4,7-trivinyl-9,9-dihexylfluorene (**3**) dissolved in $CDCl_3$. The chemical shifts are reported in ppm using tetramethylsilane (TMS) as an internal standard.

Table 1. Polymerization Results and Thermal Properties of HOFC and LOFC

polymer	M_n[a] (10^4)	M_w[a] (10^4)	PDI[a]	$\triangle H$[b] (J/g)	T_g[b] (°C)	T_d[c] (°C)	char yield[d] (wt %)
HOFC	0.50	0.84	1.6	29.4	112	382	32.5
LOFC	0.19	0.25	1.3	3.00		304	29.5

[a] Determined by gel permeation chromatography using polystyrene as standard. [b] Determined by differential scanning calorimeter (DSC) with a heating rate of 20 °C/min. [c] The temperature at 10 wt % loss in TGA thermograms. [d] The residual weight percent at 700 °C in TGA thermograms.

chloroform and toluene but also in high polar solvents such as *N*,*N*-dimethylformamide (DMF) and pyridine. Wide range of solvent choice is an advantage in the fabrication of multilayer devices. Figure 3 shows the ^1H NMR spectra of **HOPC** in which the chemical shifts at 3.8−3.3 ppm and 2.52−2.30 ppm have been assigned to the methylene protons of side crown ether moiety. The peaks located at 0.7−1.4 ppm and 2.1 ppm are ascribed to protons of pendant hexyl groups. However, the characteristic chemical shifts at 5.25−5.88 ppm indicate the existence of periphery vinyl groups from which thermally cross-linkable character can be expected.

Thermal Curing and Morphology Study. Both terminal vinyl and internal vinylene groups are reactive when subject to thermal treatment although the reactivity of the latter is much lower than the former.[31] Thermal cross-linking of the terminal vinyl groups leads to improved thermal stability. Comparing with linear counterpart (**LOFC**), hyperbranched **HOFC** owns more peripheral reactive groups which readily form as three-dimensional structure after thermal curing. This definitely reduces interchain interaction and leads to high thermal stability. Thermal curing behaviors of oligomers **HOFC** and **LOFC** were investigated by differential scanning calorimetry (DSC), as shown in Figure 4. During the first heating scan, the exothermic heat of both **HOFC** and **LOFC** starts at about 120 °C, with the maximum exotherm occurs at 180 and 190 °C, respectively. The exothermic heat is attributable to cross-linking reaction heat of the terminal vinyl groups. However, the reaction heat of **HOFC** (29.4 J/g) is much larger than that of **LOFC** (3.0 J/g), due to higher concentration of terminal vinyl groups in **HOFC**. In addition, no detectable exothermic peak was observed in the second heating scan for both **HOFC** and **LOFC**, indicating complete consumption of the vinyl groups in the first heating scan. After thermal treatment, cured **HOFC** showed a glass-transition temperature (T_g) around 112 °C, but no evident

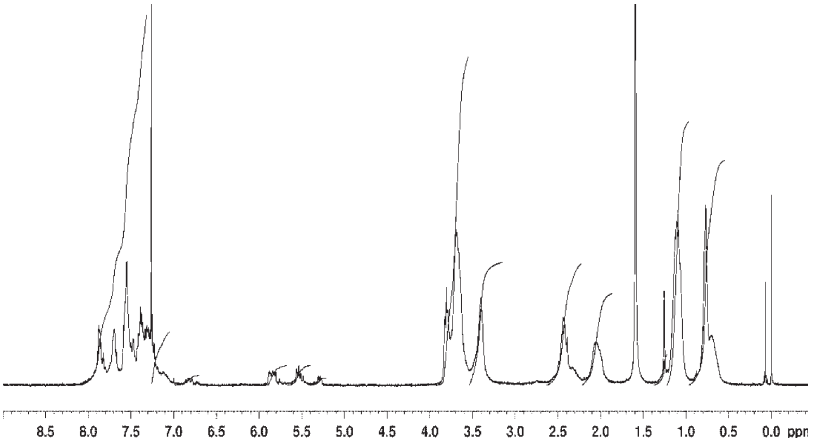

Figure 3. ^{1}H NMR spectra of hyperbranched oligo(fluorene vinylene) (**HOFC**) dissolved in $CDCl_3$. The chemical shifts are reported in ppm using tetramethylsilane (TMS) as an internal standard.

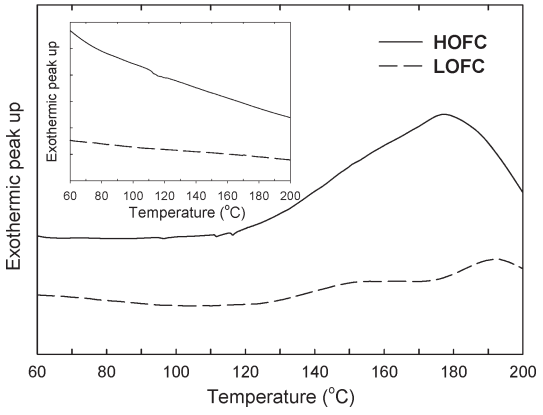

Figure 4. DSC thermograms of **HOFC** and **LOFC**. First run was used to observe the reaction heat of periphery or terminal vinyl groups of **HOFC** and **LOFC**. Inset figure shows the DSC thermograms of second heating scan (scan rate: 20 °C/min).

thermal transition was observed for cured **LOFC**. Thermal stability of the cured polymers (thermal treatment at 180 °C for 1 h) is also examined by thermogravimetric analysis (Figure S1). Thermal decomposition temperature T_d (at 10 wt % loss) of **HFC** and **LFC** are 381.5 and 303.6 °C, with the residual weight percents at 700 °C being 32.5 and 29.5%, respectively. Clearly, **HFC** exhibits better thermal stability than **LFC** due to its higher cross-linking density. However, to fabricate efficient PLED device requires not only thermal stability but also highly homogeneous film of deposited polymer. Hyperbranched polymers can improve film morphology because of their highly branched and globular structure, which decreases the interchain cohesive force to result in more stable amorphous film. Figure 5 shows 2D and 3D images of cured **HFC** and **LFC**, obtained from atomic force microscope (AFM: tapping-mode). The root-mean-square roughness of hyperbranched oligomer **HOFC** (rms = 0.83 nm) is much lower than that of linear oligomer **LOFC** (rms = 5.20 nm) and further decrease to be 0.45 and 2.35 nm for **HFC** and **LFC**, respectively, after thermal curing. Comparing to **LFC**, **HFC** exhibited more homogeneous film morphology. It can be attributed to higher molecular weight of **HOFC** or hyperbranched structure in **HFC**. However, it is well-known that hyperbranched polymers exhibit better film-forming ability, improved film morphology, and reduced crystallization, which have been ascribed to their three-dimensional structures.[22,23] To conclude, hyperbranched **HOFC** reveals thermal stability and homogeneous morphology superior to **LOFC** after thermal cross-linking. These characteristics are key factors in obtaining high-performance electroluminescent devices.

Photophysical Properties. Figure 6 shows the absorption and PL spectra of **HOFC** and **LOFC** in $CHCl_3$ and as thin films spin-coated from $CHCl_3$ solution (20 mg/mL), with the corresponding optical data summarized in Table 2. In $CHCl_3$ solution, **HOFC** and **LOFC** show absorptions peaked at 424 and 404 nm, respectively, which can be attributed to the $\pi-\pi^*$ electronic transition of the main chain. The absorption peak of **HOFC** is red-shifted 20 nm relative to that of **LOFC**, which is attributable to its longer effective conjugation length due to higher molecular weight. According to previous study,[36] oligo(fluorene vinylene)s with absorption peaks at 424 and 404 nm correspond to the oligomers with 7 and 3−4 repeat units. The fluorescence maxima of **HOFC** and **LOFC** in $CHCl_3$ are at 472 and 463 nm, respectively. In film state, the absorption peaks are located at 425 and 407 nm and the emission maxima are situated at 478 and 473 nm. The PL spectral red-shift of **LOFC** (10 nm) in going from solution to film state is larger than that of **HOFC** (6 nm). This is attributable to higher interchain interaction in **LOFC**, which is facilitated by its linear structure and polar crown ether groups. However, the smaller red-shift of hyperbranched **HOFC** is mainly due to its branched and globular molecular structure. Figure 7 shows the absorption and PL spectra of oligomers (**HOFC**, **LOFC**) and their cross-linked polymers (**HFC**, **LFC**) obtained by curing at 180 °C for 1 h under nitrogen atmosphere. Thermal treatment of polymer film possibly leads to formation of aggregate or excimer which cause shift in emission peak or change in spectral feature. This leads to a change in emission color, especially when the applying temperature is higher than the glass-transition temperature of the polymer. After the thermal treatment, the PL spectral intensity of **LFC** at longer wavelength is higher than that of **LOFC** (Figure 7b). However, the absorption and PL spectral features of **HFC** are almost identical to those **HOFC** (Figure 7a), suggesting that the photoluminescence of cured **HFC** is stable under the thermal treatment. Furthermore, solvent resistance of **HOFC** should be enhanced after thermal cross-linking. To examine solvent resistance of **HFC**, it was washed with good solvents of **HOFC** (toluene and $CHCl_3$) to investigate its absorption and PL spectral changes. Only slight intensity reduction was observed in absorption and PL spectra after the solvent washes, suggesting high solvent resistance is reached after

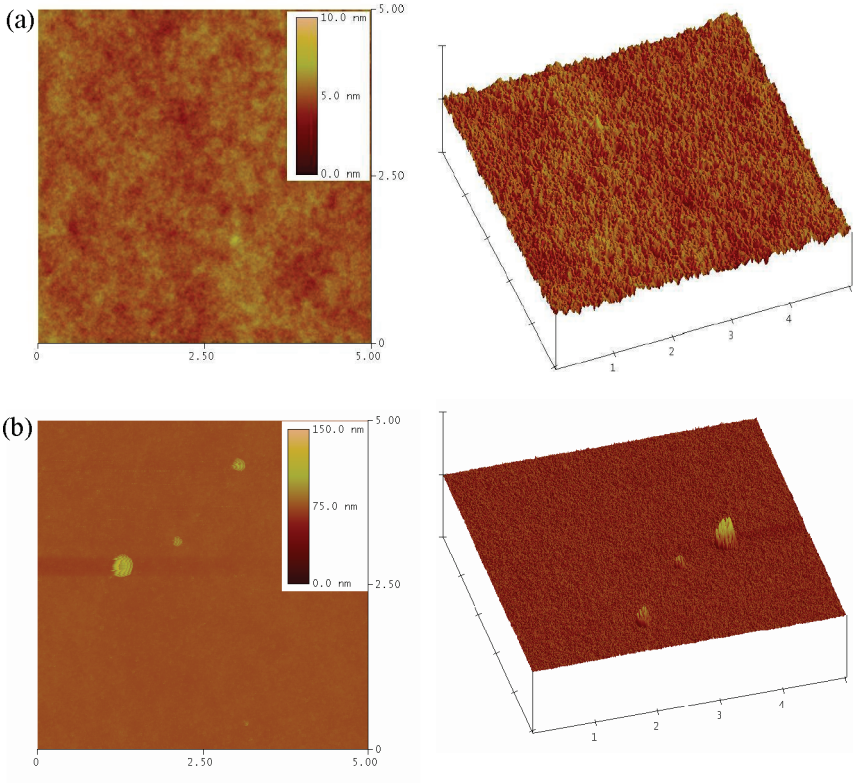

Figure 5. 2D (left) and 3D images (right) of cured **HFC** (a) and **LFC** (b). The precursor oligomers **HOFC** and **LOFC** were coated on ITO glass and cured at 180 °C for 1 h under nitrogen atmosphere (scan size: 5 × 5 μm).

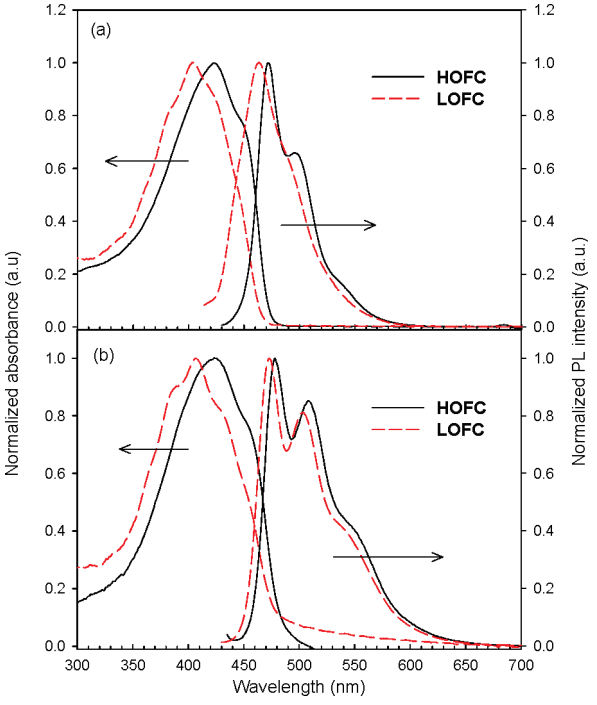

Figure 6. Absorption and photoluminescence (PL) spectra of **HOFC** and **LOFC**: (a) in $CHCl_3$ (1×10^{-5} M, excitation: 423 nm for **HOFC** and 404 nm for **LOFC**), (b) as films coated on quartz plate (spin-coated from polymer solution: 20 mg/mL. excitation: 435 and 407 nm for **HOFC** and **LOFC**, respectively).

thermal curing. This thermal cross-linking characteristic in **HOFC** is beneficial to multilayer PLED device fabrication.

Chemosensory Properties. Crown ether is commonly employed as molecular host to complex with alkali and alkaline earth metal cations, transition metal cations and ammonium cations. Combination of crown ether receptor with conjugated polymer backbone renders amplified fluorescence and absorption spectral variations in the presence of different metal ions. We attached 15-crown-4 group directly to 9-position of fluorene units to reduce the distance between recognition moiety and transducer (conjugated polyfluorene backbone). The resulting polymers (**HOFC**, **LOFC**) are multifunctional material consisting of conjugated backbone and pendant crown ether as recognition moiety. Therefore, they can be applied either as a chemical sensor for cations or as emitting material for electroluminescent devices. Fluorescence is a widely used sensing signal in chemical sensors and biosensors, that is, it offers diverse transduction schemes based on change in intensity, energy transfer, wavelength shifting, and lifetime decay. Figure 8 shows the PL spectra of oligomer **HOFC** in the presence of various cations. The PL intensity is decreased significantly in present of Fe^{3+} and Ru^{3+}, suggesting its high selectivity to these two cations. Linear oligomer **LOFC** also demonstrates identical selective response to Fe^{3+} and Ru^{3+} due to having the same crown ether as recognition moiety. The chelating capability of crown ether depends on the match of its cavity size and the diameter of the metal ions. The selectivity response is governed by the complement of cavity size of crown ether and diameter of metal ions. The diameters of Fe^{3+} and Ru^{3+} (Fe^{3+}: 1.34 Å; Ru^{3+}: 1.24 Å) are more fitted to the cavity size of the pendant crown ether. In addition, they are both trivalent ions that will bind with the crown ether to form more a stable complex than univalent and divalent ions. The PL quenching is probably caused by the crown ether-bound metal ions to which the photoexcited energy of main chain is transferred. The energy transfer is highly probable due to the proximity between bound ions and main chain. The Stern−Volmer relationship allows us to investigate the

Table 2. Photophysical Properties of HOFC and LOFC

polymer	UV−vis λ_{max} solution[a] (nm)	PL λ_{max} solution[a] (nm)	UV−vis λ_{max} film (nm)	PL λ_{max} film (nm)
HOFC	424, 452s[b]	472, 498s[b]	425, 465s[b]	478, 509
LOFC	404, 424s[b]	463	407, 433s[b]	473, 503

[a] 1×10^{-5} M in $CHCl_3$. [b] The s means the wavelength of the shoulder.

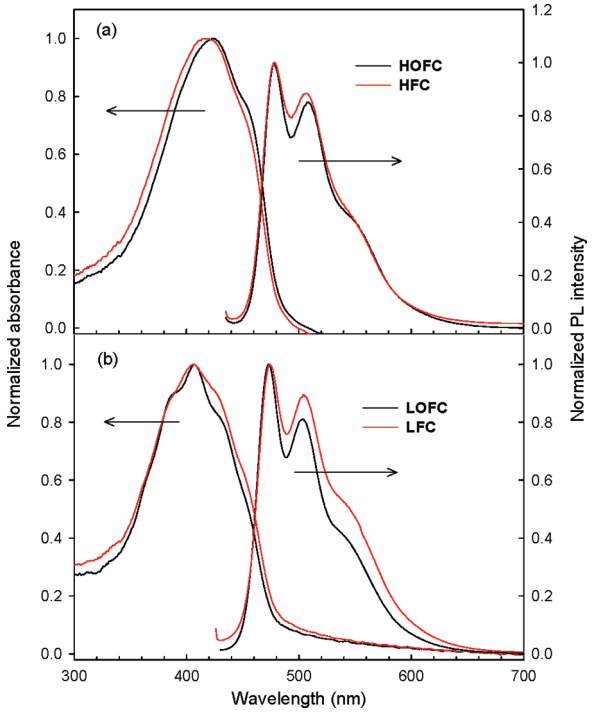

Figure 7. Absorption and PL spectra (excitation: 435 nm) of oligomers **HOFC** (a) and **LOFC** (b) before and after thermal curing at 180 °C for 1 h under a nitrogen atmosphere.

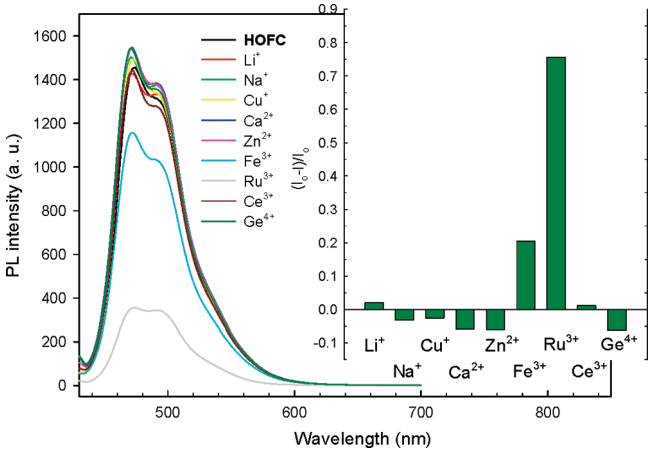

Figure 8. Photoluminescence spectra of **HOFC** in the presence of various metal cations (excitation: 423 nm). Concentration of polymer: 10^{-6} M in DMF/H_2O = 9/1 (v/v), concentration of metal ion: 2.2×10^{-4} M. Inset figure is the PL response profile by adding different metal cations.

kinetic of a photophysical intermolecular deactivation process. As shown in Figure 9, the PL intensity is decreased with an increase in concentration of Ru^{3+} cation. The Stern−Volmer plot for Ru^{3+} shows upward curvature, suggesting that the quenching is attributed to the sphere-of-action mechanism.[37−39] The Stern−Volmer constants (K_{sv}) of **HOFC** and **LOFC** toward Ru^{3+}, estimated at low

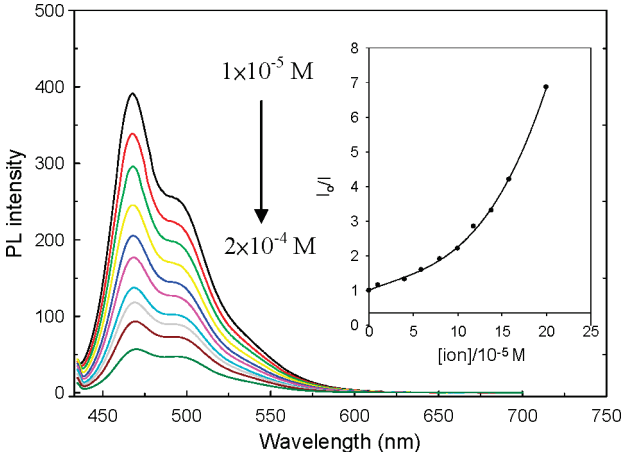

Figure 9. Photoluminescence (PL) spectra of **HOFC** in the presence of various concentration of Ru^{3+} cation (excitation: 423 nm). Concentration of polymer: 10^{-6} M in DMF/H_2O = 9/1 (v/v). Inset figure is Stern−Volmer plot of PL quenching at various concentration of Ru^{3+}.

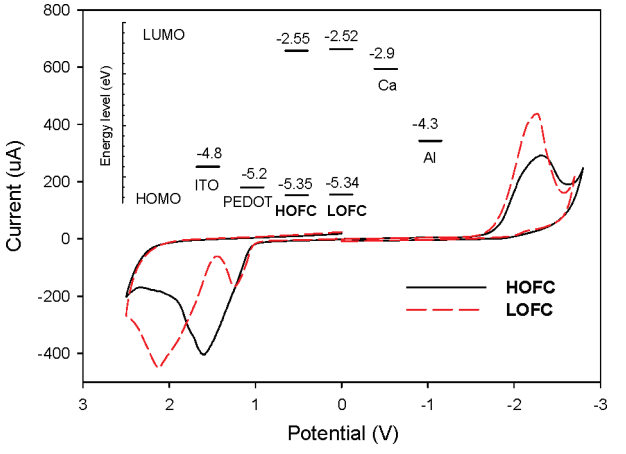

Figure 10. Cyclic voltammograms of **HOFC** and **LOFC** at a scanning rate of 100 mV/s. The inset shows energy diagrams of **HOFC**, **LOFC**, PEDOT:PSS, and electrodes.

quencher concentration (below 1.38×10^{-4} M), are 2×10^4 and 1.9×10^4 M^{-1}, respectively. The stability constant (K_s) of forming complex with Ru^{3+} are 3.1×10^3 and 5×10^3 M^{-1} for **HOFC** and **LOFC** (Figure S2), respectively. The estimation of K_{sv} and K_s is described in the Supporting Information. These results indicate that the **HOFC** and **LOFC** containing pendant crown ether are promising chemical sensor for metal cations. In recent research, hyperbranched conjugated polymers showed better sensing efficiency than linear counterparts.[30,40,41] It has been attributed to that hyperbranched conjugated polymers provide a greater number of possible exciton migration pathways through the joining of the branch unit, which increases the probability of exciton quenched by analyte.[30,40,41] However, the branching at 4-position of **HOFC** leads to a 41.6° twist angle between the two fluorene units, as shown in its optimized geometry (Figure S3: obtained from semiempirical MNDO

Table 3. Electrochemical Properties of the HOFC and LOFC

	E_{ox}v s FOC[a] (V)	E_{red} vs FOC[a] (V)	E_{HOMO}[b] (eV)	E_{LUMO}[b] (eV)	E_g[c] (eV)
HOFC	0.55	−2.25	−5.35	−2.55	2.80
LOFC	0.54	−2.28	−5.34	−2.52	2.82

[a] E_{FOC} = 0.48 V vs Ag/AgCl. [b] $E_{HOMO} = -(E_{ox,\ FOC} + 4.8\ V)$ eV; $E_{LUMO} = -(E_{red,\ FOC} + 4.8)$ eV. [c] Band gap: E_g = |LUMO − HOMO|.

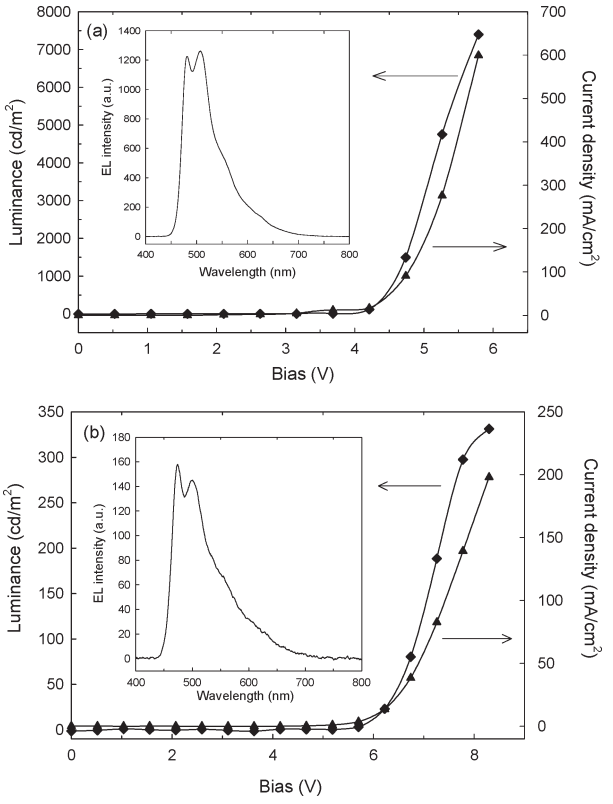

Figure 11. Current density-bias (▲) and brightness-bias (♦) characteristic of double-layer EL devices (ITO/PEDOT:PSS/polymer/Ca/Al) using cured **HFC** (a) and **LFC** (b) as emitting layer. The inset figure is the corresponding EL spectra.

calculation). This twist is unfavorable to the migration of excitons through the branch unit. Accordingly, the sensing properties of **HOFC** and **LOFC** are comparable.

Electrochemical Properties. Cyclic voltammetry has been applied and considered as an effective tool to investigate electrochemical properties of conjugated polymers. **HOFC**- or **LOFC**-coated glassy carbon was used as working electrode and immersed in anhydrous acetonitrile containing 0.1 M tetra-*n*-butylammonium perchlorate (Bu_4NClO_4) as electrolyte. Figure 10 demonstrates the cyclic voltammograms of **HOFC** and **LOFC** films. Two oxidation peaks of **LOFC** at 1.24 and 2.14 V are probably attributed to the formation of radical cation and dication, respectively. However, only one broad peak at about 1.6 V is observed in **HOFC**. This phenomenon has been attributed to electronic interaction between branches upon oxidation, which is not electronically isolated.[42] The onset oxidation potentials of **HOFC** and **LOFC** are observed at 1.03 and 1.02 V, respectively. And the reduction potentials are situated at −1.77 and −1.8 V (Table 3). The highest occupied molecular orbital (HOMO) and lowest unoccupied molecular orbital (LUMO) levels are estimated by using the equations $E_{HOMO} = -(E_{ox} + 4.8)$ eV and $E_{LUMO} = -(E_{red} + 4.8)$ eV, where E_{ox} and E_{red} are the onset reduction and oxidation potentials relative to the ferrocene/ferrocenium couple. The HOMO and LUMO energy levels of **HOFC** are −5.35 and −2.55 eV, respectively, and those of **LOFC** are −5.34 and −2.52 eV (Inset in Figure 10). Clearly, **HOFC** and **LOFC** possesses almost identical oxidation and reduction potentials, and accordingly the band gaps of **HOFC** and **LOFC** are comparable (2.80−2.82 eV) as well.

Table 4. Optoelectronic Properties of the Electroluminescent Devices[a]

sample	thickness[b] (nm)	turn-on voltage[c] (V)	maximum luminance (cd/m²)	maximum LE[d] (cd/A)	CIE 1931 (*x*, *y*)
HFC	101	4.1	7132	1.33	(0.24, 0.44)
LFC	95	6.2	331	0.22	(0.23, 0.35)

[a] Device configuration: ITO/PEDOT:PSS/**HFC** or **LFC**/Ca/Al. [b] The thickness of device was examined by atomic forcing microscopy (AFM). [c] Defined as the voltage required for the luminance at 10 cd/m². [d] Maximum luminance efficiency.

Electroluminescent Properties of LED Devices. Double-layer electroluminescent (EL) devices with a configuration of ITO/PEDOT:PSS/emitting layer/Ca(50 nm)/Al(100 nm) were fabricated to investigate their optoelectronic characteristics. Cured polymers (**HFC** and **LFC**) were used as emitting layer because of their higher homogeneity than corresponding precursors (**HOFC** and **LOFC**). The **HFC** and **LFC** films were obtained by spin-coating **HOFC** and **LOFC** solution in chlorobenzene (20 mg/mL), respectively, followed by curing at 180 °C for 1 h under a nitrogen atmosphere. Figure 11 shows current density versus bias and luminance versus bias of the EL devices, with the characteristic data summarized in Table 4. The main emission peaks are situated at 481 and 508 nm for **HFC** device (475 and 502 nm for **LFC** device), which are similar to their corresponding PL spectra in film state. The turn-on voltage of **HFC** device (4.1 V) is much lower than that of **LFC** device (6.2 V). Furthermore, the maximum luminance and maximum luminance efficiency of **HFC** device (7132 cd/m², 1.3 cd/A) are superior to those of **LFC** device (331 cd/m², 0.22 cd/A). The EL performance enhancement in **HFC** device is attributable to its improved film morphology after thermal curing as discussed in AFM study. Moreover, the maximum luminance and maximum luminance efficiency of **HFC** device are also superior to those of hyperbranched poly(fluorene vinylene) without pendant crown ether groups (2180 cd/m², 0.89 cd/A).[43] Accordingly, side crown ether groups contribute greatly to the performance enhancement. The compatibility between organic emitting layer and cathode (calcium) is promoted in the presence of polar crown ether moieties. Intimately compatible interface usually leads to decreased interfacial energy that is conducive to electron injection.[32]

Conclusion

We successfully synthesized and characterized trivinylfluorene monomer (**3**) and used it to prepare multifunctional hyperbranched (**HOFC**) containing crown ether groups via Heck coupling reaction. A corresponding linear oligo(fluorene vinylene)s (**LOFC**) was also synthesized for comparative study. Both **HOFC** and **LOFC** exhibited high selectivity toward Fe^{3+} and Ru^{3+} cations and their Stern−Volmer constants (K_{sv}) are 2×10^4 and $1.9 \times 10^4\ M^{-1}$, respectively. The stability constant (K_s) of

forming complex with Ru^{3+} are 3.1×10^3 and 5×10^3 M^{-1} for **HOFC** and **LOFC**. Cured **HFC** revealed better film homogeneity and thermal stability (rms: 0.45 nm; T_d: 382 °C) than cured **LFC** (rms: 2.3 nm; T_d: 304 °C), mainly due to its hyperbranched structure (in precursor **HOFC**) and high cross-linking density, respectively. Double-layer EL devices (ITO/PEDOT:PSS/**HFC** or **LFC**/Ca/Al) were fabricated to investigate their optoelectronic properties. The turn-on voltage, maximum luminance and maximum luminance efficiency of **HFC** device were 4.1 V, 7132 cd/m^2, and 1.3 cd/A, respectively, which is superior to those of **LFC** device (6.2 V, 331 cd/m^2, 0.22 cd/A). This EL enhancement in **HFC** device has been attributed to homogeneous film morphology after thermal curing. Present results demonstrate that hyperbranched **HOFC** is a promising candidate for both chemosensory and electroluminescent materials.

Acknowledgment. The authors thank the National Science Council of Taiwan for financial aid through Project NSC 95-2221-E006-226-MY2 and NSC 95-2221-E006-226-MY3.

Supporting Information Available: Synthesis of 2,4,7-tri-(bromomethyl)-9,9- dihexylfluorene (**1**) and 2,4,7-tri[methylene(triphenylphosphonium bromide)]-9,9-dihexylfluorene (**2**); TGA thermograms of HFC and LFC; determination of Stern−Volmer constant (K_{sv}) and stability constant (K_s); optimized geometry of **HOFC** obtained from semiempirical MNDO calculation. This material is available free of charge via the Internet at http://pubs.acs.org.

References and Notes

(1) Burroughes, J. H.; Bradley, D. D. C.; Brown, A. R.; Marks, R. N.; Mackay, K.; Friend, R. H.; Bruns, P. L.; Holmes, A. B. *Nature* **1990**, *347*, 539.
(2) Akcelrud, L. *Prog. Polym. Sci.* **2003**, *28*, 875.
(3) Satrijo, A.; Swager, T. M. *J. Am. Chem. Soc.* **2007**, *129*, 16020.
(4) Pu, K. Y.; Pan, S. Y. H.; Liu, B. *J. Phys. Chem. B* **2008**, *112*, 9295.
(5) Colladet, K.; Fourier, S.; Cleij, T. J.; Lutsen, L.; Gelan, J.; Vanderzande, D.; Nguyen, L. H.; Neugebauer, H.; Sariciftci, S.; Aguirre, A.; Janssen, G.; Goovaerts, E. *Macromolecules* **2007**, *40*, 65.
(6) Liu, C. L.; Tsai, J. H.; Lee, W. Y.; Chen, W. C.; Jenekhe, S. A. *Macromolecules* **2008**, *41*, 6952.
(7) Horowitz, G. *Adv. Mater.* **1998**, *10*, 365.
(8) Baek, N. S.; Hau, S. K.; Yip, H. L.; Acton, O.; Chen, K. S.; Jen, A. K. Y. *Chem. Mater.* **2008**, *20*, 5734.
(9) (a) Kreyenschmidt, M.; Klärner, G.; Fuhrer, T.; Ashenhurst, J.; Karg, S.; Chen, W. D.; Lee, V. Y.; Scoot, J. C.; Miller, R. D. *Macromolecules* **1998**, *31*, 1099. (b) Neher, D *Macromol. Rapid Commun.* **2001**, *22*, 1365.
(10) Chen, S. A.; Lu, H. H.; Huang, C. W. *Adv. Polym. Sci.* **2008**, *212*, 49–84.
(11) Zojer, E.; Pogantsch, A.; Hennebicq, E.; Beljonne, D.; Brédas, J. L.; Scandiucci de Freitas, P.; Scherf, U.; List, E. J. W. *J. Chem. Phys.* **2002**, *117*, 6794.
(12) Lu, H. H.; Liu, C. Y.; Jen, T. H.; Liao, J. L.; Tseng, H. E.; Huang, C. W.; Huang, M. C.; Chen, S. A. *Macromolecules* **2005**, *38*, 10829.
(13) Liu, L.; Lu, P.; Xie, Z.; Wang, H.; Tang, S.; Wang, Z.; Zhang, W.; Ma, Y. *J. Phys. Chem. B* **2007**, *111*, 10639.
(14) Miteva, T.; Meisel, A.; Knoll, W.; Nothofer, H. G.; Scherf, U.; Müller, D. C.; Meerholz, K.; Yasuda, A.; Neher, D. *Adv. Mater.* **2001**, *13*, 565.
(15) Su, H.; Wu, F. I.; Shu, C. F.; Tung, Y. L.; Chi, Y.; Lee, G. H. *J. Polym. Sci., Part A: Polym. Chem.* **2005**, *43*, 859.
(16) Takagi, K.; Kunii, S.; Yuki, Y. *J. Polym. Sci., Part A: Polym. Chem.* **2005**, *43*, 2119.
(17) Wu, C. W.; Lin, H. C. *Macromolecules* **2006**, *39*, 7232.
(18) He, Q. Y.; Lai, W. Y.; Ma, Z.; Chen, D. Y.; Huang, W. *Eur. Polym. J.* **2008**, *44*, 3169.
(19) (a) Tsai, L. R.; Li, C. W.; Chen, Y. *J. Polym. Sci., Part A: Polym. Chem.* **2008**, *46*, 5945. (b) Chen, S. H.; Shiau, C. S.; Tsai, L. R.; Chen, Y. *Polymer* **2006**, *47*, 8436. (c) Tsai, L. R.; Chen, Y. *J. Polym. Sci., Part A: Polym. Chem.* **2007**, *45*, 4465. (d) Tsai, L. R.; Chen, Y. *Macromolecules* **2007**, *40*, 2984.
(20) Wang, R.; Wang, W. Z.; Yang, G. Z.; Liu, T.; Yu, J.; Jiang, Y. *J. Polym. Sci., Part A: Polym. Chem.* **2008**, *46*, 790.
(21) Wang, P. W.; Liu, Y. J.; Devadoss, C.; Bharathi, P.; Moore, J. S. *Adv. Mater. Commun.* **1996**, *8*, 237.
(22) Peng, Q.; Yan, L.; Chen, D.; Wang, F.; Wang, P.; Zou, D. *J. Polym. Sci., Part A: Polym. Chem.* **2007**, *45*, 5296.
(23) Wang, H.; Sun, Y.; Qi, Z.; Kong, F.; Ha, Y.; Yin, S.; Lin, S. *Macromolecules* **2008**, *41*, 3537.
(24) Wen, G. A.; Xin, Y.; Zhu, X. R.; Zeng, W. J.; Zhu, R.; Feng, J. C.; Cao, Y.; Zhao, L.; Wang, L. H.; Wei, W.; Peng, B.; Huang, W. *Polymer* **2007**, *48*, 1824.
(25) Lim, S. J.; Seok, D. Y.; An, B. K.; Jung, S. D.; Park, S. Y. *Macromolecules* **2006**, *39*, 9.
(26) Klärner, G.; Lee, J. I.; Lee, V. Y.; Chan, E.; Chen, J. P.; Nelson, A.; Markiewicz, D.; Siemens, R.; Scott, J. C.; Miller, R. D. *Chem. Mater.* **1999**, *11*, 1800.
(27) Sun, H.; Liu, Z.; Hu, Y.; Wang, L.; Ma, D.; Jing, X.; Wang, F. *J. Polym. Sci., Part A: Polym. Chem.* **2004**, *42*, 2124.
(28) McQuade, D. T.; Pullen, A. E.; Swager, T. M. *Chem. Rev.* **2000**, *100*, 2537.
(29) de Silva, A. P.; Gunaraten, H. Q. N.; Gunnlaugsson, T.; Huxley, A. J. M.; McCoy, C. P.; Rademacher, J. T.; Rice, T. E. *Chem. Rev.* **1997**, *97*, 1515.
(30) Thomas, S. W.; Joly, G. D.; Swager, T. M. *Chem. Rev.* **2007**, *107*, 1339.
(31) Tsai, L. R.; Chen, Y. *J. Polym. Sci., Part A: Polym. Chem.* **2008**, *46*, 70.
(32) Yu, J. M.; Chen, Y. *J. Polym. Sci., Part A: Polym. Chem.* **2009**, *47*, 2985.
(33) Mikroyannidis, J. A.; Yu, Y. J.; Lee, S. H.; Jin, J. I. *J. Polym. Sci., Part A: Polym. Chem.* **2006**, *44*, 4494.
(34) Liu, Y.; Liu, M. S.; Jen, A. K.-Y. *Acta Polym.* **1999**, *50*, 105.
(35) Tsai, L. R.; Chen, Y. *J. Polym. Sci., Part A: Polym. Chem.* **2007**, *45*, 5541.
(36) Lin, Q.; Liu, W.; Yao, B.; Tian, H.; Xie, Z.; Geng, Y.; Wang, F. *Macromolecules* **2007**, *40*, 1851.
(37) Giri, R. *Spectrochim. Acta, Part A* **2004**, *60*, 757.
(38) Thipperudrappa, J.; Biradar, D. S.; Hanagodimath, S. M. *J. Lumin.* **2007**, *124*, 45.
(39) Suresh Kumar, H. M.; Kunabenchi, R. S.; Biradar, J. S.; Math, N. N.; Kadadevarmath, J. S.; Inamdar, S. R. *J. Lumin.* **2006**, *116*, 35.
(40) Feng, J.; Li, Y.; Yang, M. *J. Polym. Sci., Part A: Polym. Chem.* **2009**, *47*, 222.
(41) Tolosa, J.; Kub, C.; Bunz, U. H. F. *Angew. Chem., Int. Ed.* **2009**, *48*, 4610.
(42) Kanibolotsky, A. L.; Berridge, R.; Skabara, P. J.; Perepichka, I. F.; Bradley, D. D. C.; Koeberg, M. *J. Am. Chem. Soc.* **2004**, *126*, 13695.
(43) Tsai, L. R.; Chen, Y. *Macromolecules* **2008**, *41*, 5098.